# An IR Near-Field Study of the Solid Electrolyte Interphase on a Tin Electrode

**ARTICLE** *in* JOURNAL OF PHYSICAL CHEMISTRY LETTERS · MARCH 2015

Impact Factor: 7.46 · DOI: 10.1021/acs.jpclett.5b00263



**3 AUTHORS**, INCLUDING:

Maurice Ayache

Lawrence Berkeley National Laboratory

**14** PUBLICATIONS **220** CITATIONS

SEE PROFILE

Robert Kostecki

Lawrence Berkeley National Laboratory

**133** PUBLICATIONS **3,809** CITATIONS

SEE PROFILE

THE JOURNAL OF PHYSICAL CHEMISTRY Letters

Letter

pubs.acs.org/JPCL

# IR Near-Field Study of the Solid Electrolyte Interphase on a Tin Electrode

Maurice Ayache, Simon Franz Lux, and Robert Kostecki*

Energy Storage and Distributed Resources Division, Lawrence Berkeley National Laboratory, 1 Cyclotron Road, Berkeley, California 94720, United States

**ABSTRACT:** There has been a dearth of suitable techniques for studying the chemical composition of solid electrolyte interphase (SEI) on Li-ion negative electrodes at a resolution of its basic building blocks' length scale. Infrared apertureless near-field scanning optical microscopy (IR aNSOM) is an emerging tool in the chemical characterization of interfacial layers on the nanometer scale. This work demonstrates an IR aNSOM imaging of the SEI layer on a model Sn electrode. IR aNSOM images reveal significant chemical contrast variations tied to specific topographic features and possible corresponding distribution of lithium carbonate and lithium ethylene dicarbonate on the Sn electrode surface.

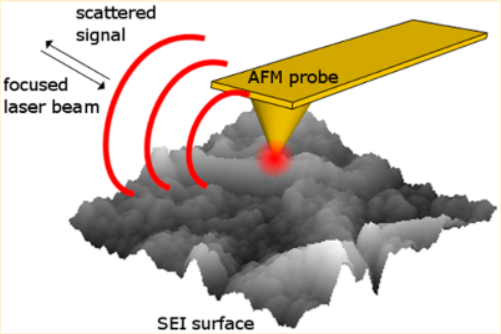


Fundamental investigations of basic properties of electrode materials and electrode/electrolyte interfaces are essential for improvements in electric energy storage systems.[1] Among the most critical aspects of Li-ion battery operation is the solid electrolyte interphase (SEI) layer,[2] which forms at the negative electrode surface due to the reduction of the electrolyte during initial charge/discharge cycles.[3,4] This highly inhomogeneous, ionically conductive, and electrically resistive film prevents further electrolyte decomposition at the electrode surface and assures long-term operation of Li-ion battery cells. The chemical composition and functional mechanisms of the SEI are not well understood due to the nonhomogeneous properties of Li-ion composite electrodes and the technical barriers associated with characterization methodologies across length and temporal scales that correspond to the SEI basic components and their function.[5]

Tin is a promising negative electrode material for Li-ion systems due to its relatively high specific capacity for lithium alloying (993 mAh/g) and fast Li diffusion rate.[6,7] However, unlike graphitic carbons that produce a functional SEI layer, Sn and other intermetallic electrode materials, for example, Si, Cu−Sn−Sb, Co−Sb, and so on, tend to form unstable surface layers in organic electrolytes, which hardly passivates the electrode surface. Moreover, the surface film repeatedly breaks apart and reforms during cycling due to large volumetric changes of $Li_xSn$ ($0 < x < 4.4$) and (re)exposure of fresh reactive surfaces to the electrolyte during alloying/dealloying processes. The topography of the SEI on Sn during initial formation and cycling in organic carbonate electrolytes has been directly observed with in situ atomic force microscopy (AFM) and spectroscopic ellipsometry.[8] However, the high-resolution AFM imaging does not reveal any direct information about the local chemical composition of surfaces. The chemical composition of the SEI on the Sn electrode has been studied with spectroscopic techniques such as Fourier transform infrared spectroscopy (FTIR)[9] and attenuated total reflectance spectroscopy (ATR),[10] which have indicated the presence of lithium alkyl carbonates $ROCO_2Li$,[9] lithium carbonate $Li_2CO_3$,[11] lithium carboxylate RCOOLi,[12] and PF-containing inorganics.[10]

Conventional FTIR spectroscopy and microscopy techniques are diffraction-limited (spatial resolution on the order of 0.5−10 $\mu$m) and provide only average chemical and structural information. Moreover, in situ spectroscopic measurements of electrochemical interfaces often lack surface specificity with the surface signal being convoluted with contributions from the electrolyte and electrode material.[13] ATR spectroscopy, which uses evanescent waves, can effectively isolate the surface IR response but still suffers from diffraction-limited lateral spatial resolution. Consequently, a standard optical spectrum of the SEI layer consists of convoluted signals from many compounds present within the relatively large sampled area, and it cannot resolve the spatial chemical inhomogeneity at the nanoscale.

Apertureless near-field scanning optical microscopy (aNSOM), which uses a metallized AFM tip in contact with the sample surface as an optical probe for high-resolution spectroscopy and imaging measurements, can overcome these limitations.[14] The AFM tip is illuminated by a focused light beam, which produces a strongly enhanced electromagnetic field at the tip apex due to the lightning rod effect.[15] A schematic depicting the principle of aNSOM operation is shown in Figure 1.

The dipole scattering at the tip is modulated by the phonon response of the sample according to[16]

**Received:** February 6, 2015
**Accepted:** March 11, 2015
**Published:** March 11, 2015





DOI: 10.1021/acs.jpclett.5b00263
J. Phys. Chem. Lett. 2015, 6, 1126−1129

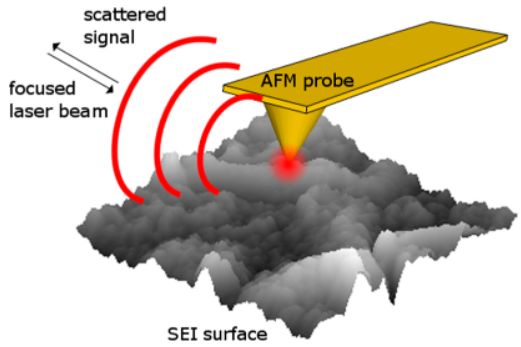


**Figure 1.** 3D schematic of aNSOM experimental setup and operational principle. A laser beam is focused onto the NSOM probe, a metallized AFM cantilever. The laser's optical field is strongly enhanced at the probe tip, and the far-field scattering is modulated by the local dielectric response of the SEI sample surface.

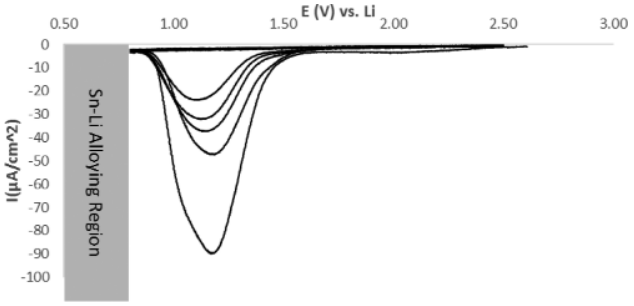


**Figure 2.** Cyclic voltammograms (CVs) of a polycrystalline Sn electrode in 1 M $LiPF_6$, EC/DEC electrolyte. Note repeated reformation of the SEI layer due to the electrolyte reduction at ~1.25 V.

$$\alpha_{\text{eff}} = \frac{\alpha(1+\beta)}{1-\alpha\beta/(16\pi(a+z)^3)} \quad (1)$$

where $\alpha$ is the polarizability of the tip metal, $\alpha_{\text{eff}}$ is the effective polarizability of the tip−sample system modeled as a metallic sphere close to a plane, $\beta = ((\varepsilon - 1)/(\varepsilon + 1))$ is the surface response function of the sample material with dielectric constant $\varepsilon$, $a$ is the tip apex radius of curvature, and $z$ is the tip−sample distance. The effective polarizability incorporates both the properties of the tip and sample surface, meaning that the instrument must be operated far from any electromagnetic resonance of the tip to present an accurate measurement of the surface optical response. Because the distance dependence of the effective polarizability is highly nonlinear, it allows lock-in amplitude and phase signal detection at higher harmonics of the tip mechanical resonance frequency for background reduction. The structural and compositional specificity of IR near-field spectroscopy and microscopy is analogous to far-field vibrational spectroscopies.[17] The unique capability of infrared near-field microscopy combined with FTIR spectroscopy to map phases distributions in microcrystals of $Li_xFePO_4$ has been demonstrated very recently.[18]

To prepare the sample, a disc-shaped tin electrode of diameter 13 mm and thickness 5 mm, was hydraulically pressed from a Sn-foil (Sigma-Aldrich, 99.9% pure, metal basis), then polished to a mirror-like finish with alumina slurry and diamond paste. The electrode was placed in a beaker cell equipped with high-purity Li-foil counter and reference electrodes and filled with 1 mol/L $LiPF_6$ in ethylene carbonate (EC)/diethyl carbonate (DEC) 1:2 (wt %) electrolyte. The Sn electrode potential was scanned five times between open-circuit potential (OCP), ~3.0 and 0.8 V versus $Li/Li^+$, that is, above the Sn−Li alloying potential region. All sample preparations and electrochemical measurements were carried out in a He-filled glovebox (Nexus II, VAC). After cycling was completed,

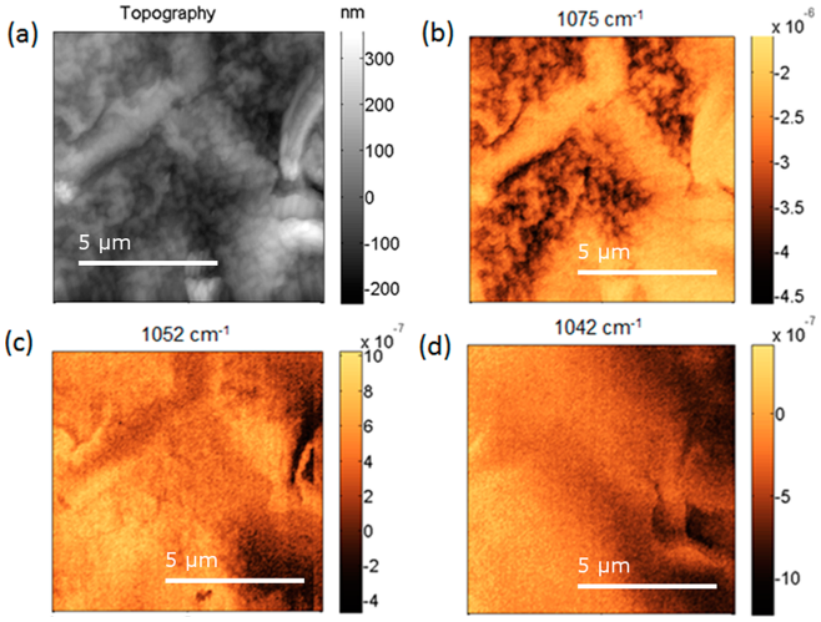


**Figure 3.** (a) Exemplary topography of region on tin SEI. (b−d) Near-field IR absorption maps over same region at wavenumbers chosen to demonstrate variation in contrast. Absorption is given by optical field imaginary component $A \sin \phi$. Sample is produced by cycling Sn 5 times from OCP ~2.7 V to 0.8 V against metallic Li without lithiation. The SEI film developed on the surface is rough, porous, and inhomogeneous. Variations in contrast are tied to specific topographic features, indicating varying chemical composition between those features.



DOI: 10.1021/acs.jpclett.5b00263
J. Phys. Chem. Lett. 2015, 6, 1126−1129

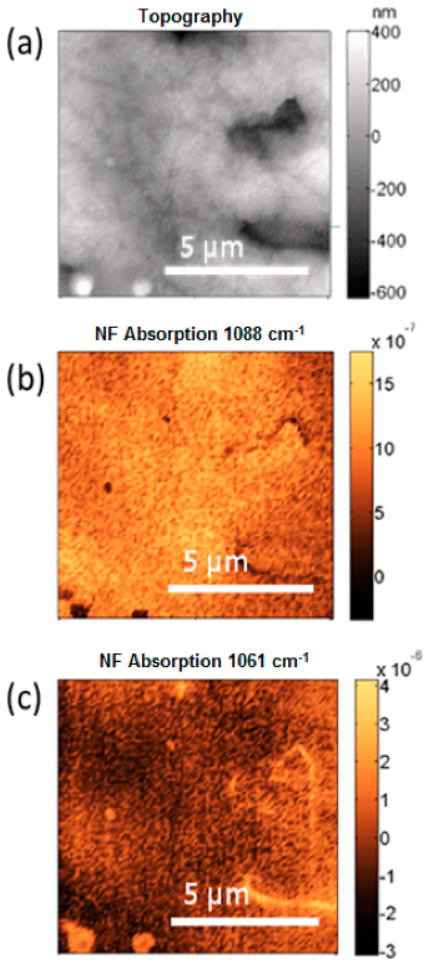


**Figure 4.** (a) Topography of region of SEI surface. (b) Near-field IR absorption map at lithium carbonate peak 1088 $cm^{-1}$. (c) Near-field IR absorption map at lithium ethylene dicarbonate peak 1061 $cm^{-1}$. Absorption is given by optical field imaginary component $A$ sin $\phi$.

the tin electrode was removed from the cell at OCP, briefly soaked in DEC to remove the electrolyte residue, dried under helium, and then placed under the IR aNSOM for surface analysis.

The current response of the Sn electrode during electrochemical cycling is shown in Figure 2. The large cathodic peak at ~1.3 V is associated with the reduction of the electrolyte and the formation of a surface film.[8] The continuous reformation of the SEI with each cycle is clearly visible with the significant charge consumed under this current peak. Even without volumetric changes associated with Sn−$Li_x$ alloying/dealloying, the SEI layer keeps growing gradually with cycling and the tin surface is never completely passivated.[8]

The cycled tin electrode surface was characterized ex situ using a Neaspec NeaSNOM aNSOM system, with a set of Daylight Solutions quantum cascade tunable IR lasers (tuning range 927−1094 $cm^{-1}$) as the light excitation source. The system is configured as a pseudoheterodyne Michelson interferometer[19] with the path length of the reference arm modulated with a piezo-actuated mirror at a frequency $f_{het} \approx$ 300 Hz. This allows recovery of the near-field optical amplitude $A$ and phase $\phi$, which are essential for measuring the local absorption, previously shown to be proportional to $A$ sin $\phi$.[20] Furthermore, the lock-in frequency is set to recover the second harmonic of the probe's mechanical resonance, which significantly reduces the background from the probe shaft due to the highly nonlinear tip−sample interaction.[19] Thus, the full lock-in detection frequency is $f = f_{het} + 2f_0$, where $f_0$ is the mechanical resonance frequency of the probe.

The cycled tin electrode surface was examined with the IR aNSOM at a variety of wavelengths over the IR spectrum to reveal inhomogeneity and chemical contrast of the SEI layer. Figure 3 shows IR near-field images, depicting the imaginary component $A$ sin $\phi$ of the same area of the tin surface taken at a set of wavelengths chosen to exemplify the observed optical contrast. Figure 3a displays the standard AFM topography image of the SEI layer on Sn. The topography of this image remains consistent during the AFM and aNSOM scans, indicating that the mechanical damage inflicted in the film by the AFM probe is minimal. Although images from only one location are shown here, they are representative for the entire SEI layer.

The observed SEI layer's surface morphology is rough, nonuniform, and porous, consistent with previous AFM results.[8] Interestingly, the contrast in the corresponding IR aNSOM images in Figures 3b−d shows a direct correlation of specific features in the topography to chemical or structural properties, which vary according to the IR aNSOM images at different wavenumbers. For instance, the three-armed structure highlighted at 1075 $cm^{-1}$ in Figure 3b undergoes a contrast inversion in Figure 3c at 1053 $cm^{-1}$ and disappears completely at 1042 $cm^{-1}$. The roughness surrounding this structure is visible at 1075 $cm^{-1}$ but does not appear at other wavenumbers. The IR aNSOM image at 1042 $cm^{-1}$ has minimal contrast except for the small surface feature in the lower right.

This variation in IR optical contrast indicates changes in the relative IR absorption due to the tip−sample dipole-phonon coupling. The local IR near-field absorption at specific frequencies represents the chemical and structural properties that are characteristic of the compounds present in the sampled area (~20 nm). Therefore, these high-resolution IR images provide very strong evidence of a nonuniform chemical composition across the sample surface, which has been suggested in literature but never shown on the nanometer length-scale. However, although these images provide a unique insight into the inhomogeneity of the SEI layer on Sn, they alone cannot be conclusively used to identify specific chemical compounds and to map their distribution as the employed imaging wavelengths do not correspond to unique spectral features of possible reference compounds.

To examine the distribution of specific compounds, we operated the IR aNSOM at specific wavelengths corresponding to far-field IR absorption peaks for selected reference compounds, which have already been detected in the SEI layer. The IR aNSOM image of the Sn surface at 1088 $cm^{-1}$ (Figure 4b), which corresponds to a C−O symmetric stretch far-field FTIR absorption peak of lithium carbonate, shows a fairly uniform near-field absorption signal intensity distribution over the surface, with the exception of the two pits on the right and the mounds in the lower left.

Studies on the surface film formed on Ni electrodes have identified lithium ethylene dicarbonate (LEDC),[21] itself a dimer of lithium alkyl carbonates $ROCO_2Li$ already identified on Sn electrodes. LEDC exhibits an O−C−O symmetric stretch peak at 1061 $cm^{-1}$ in the far-field FTIR absorption spectra. The corresponding IR aNSOM image at 1061 $cm^{1}$ (Figure 4c) shows a near-total optical contrast inversion with


DOI: 10.1021/acs.jpclett.5b00263
J. Phys. Chem. Lett. 2015, 6, 1126−1129

respect to the lithium carbonate, with bright spots indicating the presence of LEDC in the pits to the right and the mound structures on the lower left. Conversely, the cavity near the top section of the image seems to contain a high concentration of LEDC but displays no contrast for lithium carbonate. It should be noted that without full IR absorption spectra collected at each point of the IR aNSOM image the identifications of these compounds are still tentative.

Near-field optical probing of interfaces and interphases is an emerging area of electrochemical material characterization with the possibility to yield valuable information about the structure of surface layers and the functions of their chemical constituents. Although much of the work in near-field IR imaging has been on model systems, this work contributes to the growing body of work applying it to real measurements of functional materials and, in particular, to multicomponent composite materials systems. This preliminary ex situ IR aNSOM study reveals the distribution of compounds in the solid electrolyte interphase on the Sn electrode on the nanometer length scale. These results demonstrate for the first time that near-field optical spectroscopy and imaging techniques can become an exciting new class of characterization tools for probing electrochemical interfaces and surface layers, allowing tentative identification of the nanoscale distribution of chemical compounds on the SEI layer basic building block length scale. Future efforts in this area include in situ measurements of the SEI structure, morphology, and composition and possibly determining the exact function of the chemical or structural components within the SEI film.

## AUTHOR INFORMATION


### Corresponding Author

*E-mail: r_kostecki@lbl.gov.


### Notes

The authors declare no competing financial interest.

## ACKNOWLEDGMENTS

This work was supported by the Assistant Secretary for Energy Efficiency and Renewable Energy, Office of Vehicle Technologies of the U.S. Department of Energy under contract no. DE-AC02-05CH11231 under the Advanced Battery Materials Research (BMR) Program.

## REFERENCES


(1) "Basic Research Needs for Electrical Energy Storage," Report of the Basic Energy Sciences Workshop on Electrical Energy Storage, April 2−4, 2007. http://science.energy.gov/~/media/bes/pdf/reports/files/ees_rpt.pdf.

(2) Peled, E. The Electrochemical Behavior of Alkali and Alkaline Earth Metals in Nonaqueous Battery Systems the Solid Electrolyte Interphase Model. *J. Electrochem. Soc.* **1979**, *126*, 2047−2051.

(3) Aurbach, D.; Ein-Ely, Y.; Zaban, A. The Surface Chemistry of Lithium Electrodes in Alkyl Carbonate Solutions. *J. Electrochem. Soc.* **1994**, *141*, 10−12.

(4) Möller, K.-C.; Santner, H. J.; Kern, W.; Yamaguchi, S.; Besenhard, J. O.; Winter, M. In Situ Characterization of the SEI Formation on Graphite in the Presence of a Vinylene Group Containing Film-Forming Electrolyte Additives. *J. Power Sources* **2003**, *119−121*, 561−566.

(5) Winter, M. The Solid Electrolyte Interphase − The Most Important and the Least Understood Solid Electrolyte in Rechargeable Li Batteries. *Z. Phys. Chem.* **2009**, *223*, 1395−1406.

(6) Inaba, M.; Uno, T.; Tasaka, A. Irreversible Capacity of Electrodeposited Sn Thin Film Anode. *J. Power Sources* **2005**, *146*, 473−477.

(7) Yang, S.; Zavalij, P. Y.; Whittingham, M. S. Anodes for Lithium Batteries: Tin Revisited. *Electrochem. Commun.* **2003**, *5*, 587−590.

(8) Lucas, I. T.; Pollak, E.; Kostecki, R. In Situ AFM Studies of SEI Formation at a Sn Electrode. *Electrochem. Commun.* **2009**, *11*, 2157−2160.

(9) Li, J.-T.; Chen, S.-R.; Fan, X.-Y.; Huang, L.; Sun, S.-G. Studies of the Interfacial Properties of an Electroplated Sn Thin Film Electrode/Electrolyte Using in Situ MFTIRS and EQCM. *Langmuir* **2007**, *23*, 13174−13180.

(10) Song, S.-W.; Baek, S.-W. Surface Layer Formation on Sn Anode: ATR FTIR Spectroscopic Characterization. *Electrochim. Acta* **2009**, *54*, 1312−1318.

(11) Qiao, R.; Lucas, I. T.; Karim, A.; Syzdek, J.; Liu, X.; Chen, W.; Persson, K.; Kostecki, R.; Yang, W. Distinct Solid-Electrolyte-Interphases on Sn (100) and (001) Electrodes Studied by Soft X-Ray Spectroscopy. *Adv. Mater. Interfaces* **2014**, *1*, 1300115.

(12) Park, S.; Heon Ryu, J.; Oh, S. M. Passivating Ability of Surface Film Derived from Vinylene Carbonate on Tin Negative Electrode. *J. Electrochem. Soc.* **2011**, *158*, A498.

(13) Aurbach, D. The Surface Chemistry of Lithium Electrodes in Alkyl Carbonate Solutions. *J. Electrochem. Soc.* **1994**, *141*, L1.

(14) Keilmann, F.; Hillenbrand, R. Near-Field Microscopy by Elastic Light Scattering from a Tip. *Philos. Trans.: Math., Phys. Eng. Sci.* **2004**, *362*, 787−805.

(15) McLeod, A. S.; Kelly, P.; Goldflam, M. D.; Gainsforth, Z.; Westphal, a. J.; Dominguez, G.; Thiemens, M. H.; Fogler, M. M.; Basov, D. N. Model for Quantitative Tip-Enhanced Spectroscopy and the Extraction of Nanoscale-Resolved Optical Constants. *Phys. Rev. B* **2014**, *90*, 085136.

(16) Knoll, B.; Keilmann, F. Near-Field Probing of Vibrational Absorption for Chemical Microscopy. *Nature* **1999**, *399*, 7−10.

(17) Huth, F.; Govyadinov, A.; Amarie, S.; Nuansing, W.; Keilmann, F.; Hillenbrand, R. Nano-FTIR Absorption Spectroscopy of Molecular Fingerprints at 20 nm Spatial Resolution. *Nano Lett.* **2012**, *12*, 3973−3978.

(18) Lucas, I. T.; Mcleod, A. S.; Syzdek, J. S.; Middlemiss, D. S.; Grey, C. P.; Basov, D. N.; Kostecki, R. IR Near-Field Spectroscopy and Imaging of Single $Li_xFePO_4$ Microcrystals. *Nano Lett.* **2015**, *15*, 1−7.

(19) Ocelic, N.; Huber, A.; Hillenbrand, R. Pseudoheterodyne Detection for Background-Free Near-Field Spectroscopy. *Appl. Phys. Lett.* **2006**, *89*, 101124.

(20) Govyadinov, A. A.; Amenabar, I.; Huth, F.; Carney, P. S.; Hillenbrand, R. Quantitative Measurement of Local Infrared Absorption and Dielectric Function with Tip-Enhanced Near-Field Microscopy. *J. Phys. Chem. Lett.* **2013**, *4*, 1526−1531.

(21) Zhuang, G. V.; Xu, K.; Yang, H.; Jow, T. R.; Ross, P. N. Lithium Ethylene Dicarbonate Identified as the Primary Product of Chemical and Electrochemical Reduction of EC in 1:2 M $LiPF_6$/EC:EMC Electrolyte. *J. Phys. Chem. B* **2005**, *109*, 17567−17573.




DOI: 10.1021/acs.jpclett.5b00263
*J. Phys. Chem. Lett.* 2015, 6, 1126−1129